The X-Ray Structure of the Haloalcohol Dehalogenase HheA from Arthrobacter sp. Strain AD2

Jong, René M. de; Kalk, Kor H.; Tang, Lixia; Janssen, Dick B.; Dijkstra, Bauke W.

Published in:
Journal of Bacteriology

DOI:
10.1128/JB.01866-05

JOURNAL OF BACTERIOLOGY, June 2006, p. 4051–4056 Vol. 188, No. 11
0021-9193/06/$08.00+0 doi:10.1128/JB.01866-05

The X-Ray Structure of the Haloalcohol Dehalogenase HheA from *Arthrobacter* sp. Strain AD2: Insight into Enantioselectivity and Halide Binding in the Haloalcohol Dehalogenase Family

René M. de Jong,[1]† Kor H. Kalk,[1] Lixia Tang,[2] Dick B. Janssen,[2] and Bauke W. Dijkstra[1]*

Laboratory of Biophysical Chemistry[1] *and Laboratory of Biochemistry,*[2] *Groningen Biomolecular Sciences and Biotechnology Institute, University of Groningen, Nijenborgh 4, 9747 AG Groningen, The Netherlands*

Received 7 December 2005/Accepted 17 March 2006

Haloalcohol dehalogenases are bacterial enzymes that cleave the carbon-halogen bond in short aliphatic vicinal haloalcohols, like 1-chloro-2,3-propanediol, some of which are recalcitrant environmental pollutants. They use a conserved Ser-Tyr-Arg catalytic triad to deprotonate the haloalcohol oxygen, which attacks the halogen-bearing carbon atom, producing an epoxide and a halide ion. Here, we present the X-ray structure of the haloalcohol dehalogenase $HheA_{AD2}$ from *Arthrobacter* sp. strain AD2 at 2.0-Å resolution. Comparison with the previously reported structure of the 34% identical enantioselective haloalcohol dehalogenase HheC from *Agrobacterium radiobacter* AD1 shows that $HheA_{AD2}$ has a similar quaternary and tertiary structure but a much more open substrate-binding pocket. Docking experiments reveal that $HheA_{AD2}$ can bind both enantiomers of the haloalcohol substrate 1-*p*-nitrophenyl-2-chloroethanol in a productive way, which explains the low enantiopreference of $HheA_{AD2}$. Other differences are found in the halide-binding site, where the side chain amino group of Asn182 is in a position to stabilize the halogen atom or halide ion in $HheA_{AD2}$, in contrast to HheC, where a water molecule has taken over this role. These results broaden the insight into the structural determinants that govern reactivity and selectivity in the haloalcohol dehalogenase family.

Dehalogenases are enzymes that cleave carbon-halogen bonds (6). Over the years, detailed structural information has become available for several dehalogenases belonging to evolutionary unrelated families (3). One such family, which was recently characterized, comprises haloalcohol dehalogenases (4, 18, 21). The enzymes from this family were isolated from bacteria that are able to grow on vicinal haloalcohols, like 1,3-dichloro-2-propanol and 2,3-dichloro-1-propanol, or compounds that are degraded via haloalcohols, some of which are notable environmental pollutants. These dehalogenases catalyze the intramolecular substitution of the halogen atom of the haloalcohol function by the neighboring hydroxyl group, thereby producing an epoxide and a halide ion (Fig. 1A). The epoxide product can subsequently be hydrolyzed by an epoxide hydrolase, yielding the corresponding 1,2-diol (14).

Until now, six different haloalcohol dehalogenases, which can be grouped into the three subtypes (A, B, and C) on the basis of amino acid sequence similarities, have been isolated (21). Their sequences also indicated that they all are evolutionarily related to the large family of NAD(P)(H)-dependent short-chain dehydrogenases/reductases (SDRs) (21), which use a similar Ser-Tyr-Lys/Arg catalytic triad to catalyze various alcohol-ketone conversions (11). Crystallographic analysis of the haloalcohol dehalogenase HheC from *Agrobacterium radiobacter* AD1 revealed that the tyrosine residue of the conserved Ser-Tyr-Arg catalytic triad is in a position to activate the hydroxyl group of the haloalcohol function for nucleophilic attack on the vicinal halogen-bearing carbon atom (Fig. 1B) (4). The halogen atom is bound in a spacious halide-binding site, which also stabilizes the halide product. Structure comparison of the C-type haloalcohol dehalogenase HheC and the SDRs suggested that the different dehalogenase subtypes likely originated from NADH-dependent, rather than NADPH-dependent, SDR precursors (4). The different subtypes show marked differences in their catalytic behaviors: HheC is highly enantioselective towards various aliphatic and aromatic substrates (5, 8), whereas the A- and B-type dehalogenases have only a modest enantiopreference (20, 21).

Until now, structural information on the A- or B-type enzymes has not been available. Here we present the 2.0-Å-resolution crystal structure of the A-type haloalcohol dehalogenase $HheA_{AD2}$ from the 3-chloro-1,2-propanediol-utilizing *Arthrobacter* sp. strain AD2. The structure reveals an active site, which, in contrast to HheC, appears capable of binding both enantiomers of a haloalcohol substrate in a productive conformation. Furthermore, a structure comparison shows that the A- and C-type enzymes use different interactions to stabilize the halogen atom and halide ion during the catalytic cycle.

MATERIALS AND METHODS

Haloalcohol dehalogenase $HheA_{AD2}$ was purified as published elsewhere (20, 21). Crystals of $HheA_{AD2}$ were obtained from 2 μl hanging drops consisting of equal amounts of protein solution (8 mg/ml) and well solution containing 22% (wt/vol) polyethylene glycol 8000 as the precipitant, 100 mM MES [2-(*N*-morpholino)ethanesulfonic acid] buffer, pH 6.5, 100 mM magnesium acetate, and 50 mM sodium formate. Plates of dimensions of 1 by 2 by 0.2 mm^3 were observed after half a year.

A diffraction data set was collected at a wavelength of 0.93 Å at beamline

* Corresponding author. Mailing address: Laboratory of Biophysical Chemistry, Groningen Biomolecular Sciences and Biotechnology Institute, University of Groningen, Nijenborgh 4, 9747 AG Groningen, The Netherlands. Phone: 31-50-3634381. Fax: 31-50-3634800. E-mail: B.W.Dijkstra@rug.nl.

† Present address: Department of Chemistry, Columbia University, 3000 Broadway MC3153, New York, NY 10027.

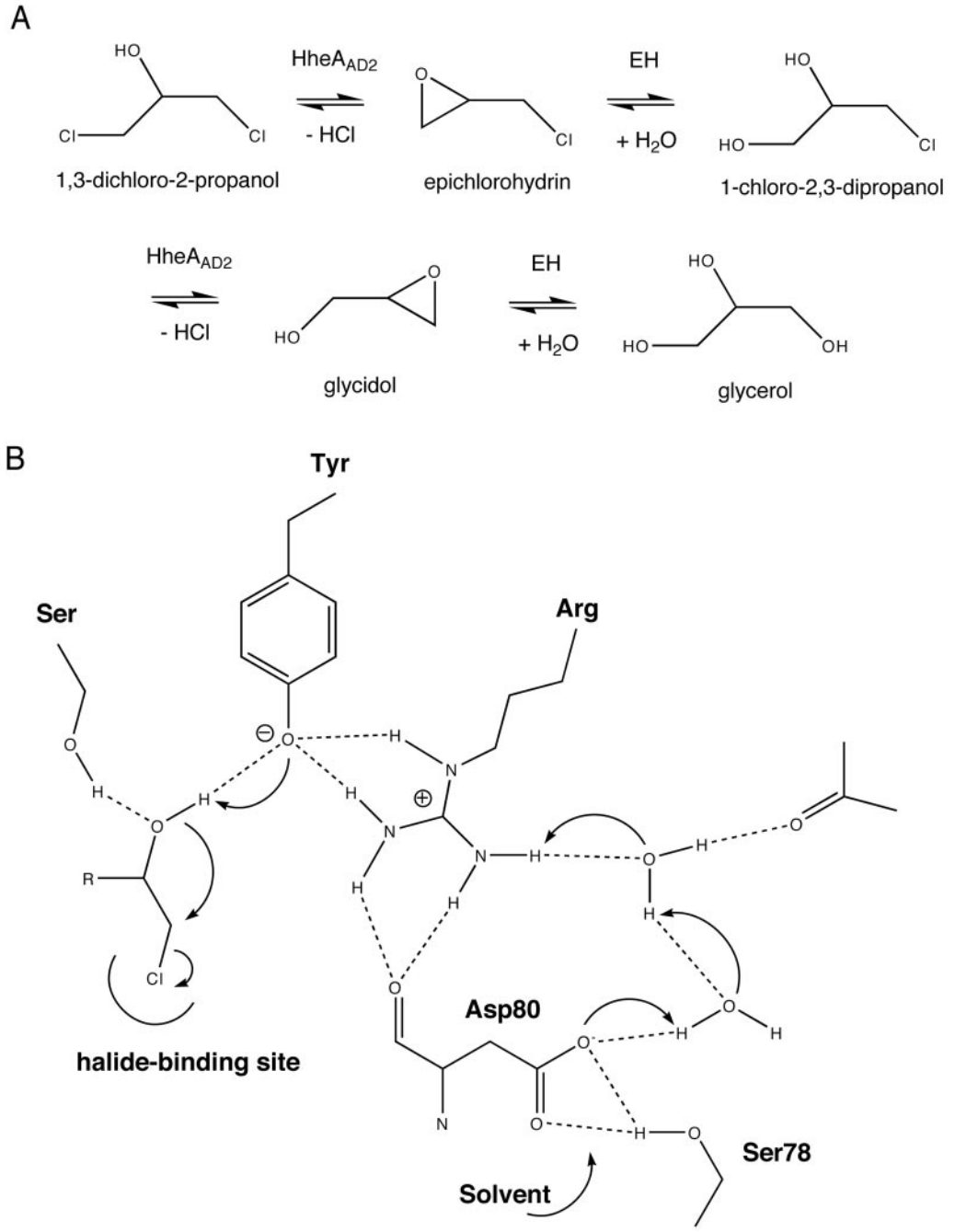

FIG. 1. (A) Putative degradation route of 1,3-dichloro-2-propanol in *Arthrobacter* sp. strain AD1. The epoxide hydrolysis step is catalyzed by epoxide hydrolase (EH), whereas the dehalogenation steps are catalyzed by the haloalcohol dehalogenase HheA$_{AD2}$. (B) Catalytic mechanism of haloalcohol dehalogenases HheC and HheA$_{AD2}$. The hydroxyl function of a haloalcohol substrate is bound by a serine (Ser134 in HheA$_{AD2}$ or Ser132 in HheC) and a tyrosine (Tyr147 in HheA$_{AD2}$ or Tyr145 in HheC). The tyrosine functions as the catalytic base, which activates the hydroxyl group adjacent to the halogen atom for nucleophilic attack on the halogen-bearing carbon atom. The abstracted proton is released to the solvent via the arginine (Arg151 in HheA$_{AD2}$ or Arg149 in HheC), the water molecules, and Asp80 at the surface of both enzymes.

ID14-2 of the ESRF synchrotron (Grenoble, France). The data were processed using DENZO and SCALEPACK (12). The crystal diffracted to 2.0-Å resolution and had space group P1 with cell dimensions of $a = 65.0$ Å, $b = 79.6$ Å, and $c = 111.5$ Å and $\alpha = 97.1°$, $\beta = 90.4°$, and $\gamma = 115.9°$, with two tetramers (each with a molecular mass of 4 × 26 kDa) in the asymmetric unit.

Molecular replacement solutions were obtained with the program AMoRe available in CCP4 (2, 10), using diffraction data between 8- and 4-Å resolution. As a search model, the atomic coordinates of the tetrameric HheC from *A. radiobacter* AD1 (PDB code 1PWX [4]) were used. Rigid body refinement of the solutions gave a starting correlation coefficient of 0.73 and an *R* factor of 32.2%. A σ_A-weighted $2F_o - F_c$ difference Fourier map (13) calculated at this stage was used in a combined NCS averaging, density modification, and phase extension procedure using the prime-and-switch method available in the program RESOLVE (19). This improved the overall figure of merit from 0.34 to 0.48 in the final cycle of the density modification procedure, and the resulting σ_A-weighted electron density maps showed improved electron density for the amino

TABLE 1. Data collection and refinement statistics

Parameter[a]	Result for native $HheA_{AD2}$
Data statistics	
Space group	P1
No. of tetramers/a.u. (no. of chains/a.u.)	2 (8)
Unit cell	a = 65.0 Å, b = 77.7 Å, c = 111.4 Å; α = 97.3°, β = 89.9°, γ = 113.0°
Resolution (Å)	20-2.0
R_{sym} (%) overall (outer shell)[b]	7.5 (28.8)
Completeness (%) overall (outer shell)	87.9 (86.6)
I/σ overall (outer shell)[b]	11.1 (3.0)
Total reflections (unique)	985,459 (120,343)
Refinement	
Total atoms/water molecules	5,438/882
R/R_{free}[c]	21.8/27.3
RMSD bonds (Å)/angles (°)	0.02/1.98
RMSD B factors (Å^2) (main chain/side chain)	0.89/1.34
Ramachandran plot (%) (fav./all./gen.all./disall.)	98.3/9.7/0.5/0.5

[a] Abbreviations: a.u., asymmetric unit; RMSD, root mean square deviation; fav., favored; all., allowed; gen. all., generously allowed; disall., disallowed.

[b] $R_{sym} = \Sigma I - <I>/\Sigma I$, where I is the observed intensity and $<I>$ the average intensity. σ, standard deviation.

[c] R, R based on 95% of the data used in refinement; R_{free}, R based on 5% of the data withheld for the cross-validation test.

acid side chains of $HheA_{AD2}$. Manual rebuilding of the structure was subsequently alternated with simulated annealing and minimization runs in CNX (Accelrys Inc., San Diego, Calif.). RESOLVE was used to obtain the most unbiased maps for model building, until σ_A-weighted $2F_o-F_c$ maps were of superior quality. The structure was built using QUANTA (Accelrys Inc., San Diego, Calif.) and XtalView (9). The quality of the final model of $HheA_{AD2}$ was analyzed with PROCHECK (7). Docking experiments were done manually in the program XtalView (9) by using the crystal structure of HheC complexed with the haloalcohol mimic (*R*)-1-para-nitrophenyl-2-azidoethanol (PDB code 1PXO) as a template. Atomic models of (*R*)- and (*S*)-1-para-nitrophenyl-2-chloroethanol were built and minimized using QUANTA. A summary of the refinement statistics and geometric quality of the models is given in Table 1. Structure-based sequence alignment of $HheA_{AD2}$ and HheC was performed with the program SEQUOIA (1).

Protein structure accession number. The coordinates and structure factor amplitudes of the haloalcohol dehalogenase $HheA_{AD2}$ have been deposited with the Protein Data Bank under accession number 1ZMO.

RESULTS AND DISCUSSION

Overall structure of HheA. Like the previously characterized haloalcohol dehalogenase HheC from *A. radiobacter* AD1 (4), $HheA_{AD2}$ from *Arthrobacter* sp. strain AD2 is a tetramer with 222 symmetry (Fig. 2A), consisting of four identical 26-kDa subunits with a Rossmann fold (15). Although their amino acid sequences are only 35% identical, the structures of the $HheA_{AD2}$ and HheC monomers are very similar and superimpose with a root mean square deviation (RMSD) of 1.3 Å for 234 Cα atoms. One of the most conspicuous differences in the overall structure of $HheA_{AD2}$ is the absence of the C-terminal extension that donates a tryptophan residue (Trp249) to the active site of a neighboring subunit in HheC (Fig. 2B). Other, more subtle structural differences are present in the loops that shape the substrate-binding pocket and the halide-binding site (see below).

Substrate-binding pocket of $HheA_{AD2}$. The active site of $HheA_{AD2}$ is located in a loop-rich region near the tip of the fourth strand of the central parallel β-sheet of the Rossmann fold. This strand contributes Ser134 of the Ser-Tyr-Arg catalytic triad (Fig. 2C). Tyr147 and Arg151 of the catalytic triad are located in adjacent turns of one of the two long α-helices that form one of the dimer interfaces in the HheA tetramer. Like in HheC, Arg151 is hydrogen bonded to the catalytic base Tyr147 and to one of two buried water molecules that are thought to relay the abstracted proton to the surface residue Asp80 (Fig. 1B) (4). Thus, $HheA_{AD2}$ and HheC use the same catalytic machinery to generate the transient oxyanion nucleophile that substitutes the vicinal halogen of a bound haloalcohol substrate during catalysis.

The most notable difference between the active sites of $HheA_{AD2}$ and HheC is the much more open structure of the substrate-binding pocket of $HheA_{AD2}$ (Fig. 2C and D). This is partly due to the absence of the C-terminal extension in $HheA_{AD2}$, which precludes the contribution of a residue from a neighboring subunit to the active site, such as Trp249 does in HheC. Another important contribution to the openness of the active site is the presence of a leucine at position 141, whereas HheC has a tryptophan (Trp139) at the equivalent position. Mutation of Trp139 into a phenylalanine previously demonstrated that the voluminous tryptophan side chain is the main determinant of the high enantioselectivity of HheC (16). Manual docking of the *R*- and *S*-enantiomers of the haloalcohol substrate 1-*p*-nitrophenyl-2-chloroethanol in the active site of $HheA_{AD2}$ shows that both enantiomers can be accommodated without severe clashes (Fig. 2C). This is in agreement with the lack of enantiopreference of $HheA_{AD2}$ (21).

Halide-binding site of HheA. Like HheC, $HheA_{AD2}$ contains a spacious halide-binding site. A water molecule is bound in the center of it, occupying a position equivalent to that of the halide ions in the structures of two product complexes of HheC (4). Such an *apo* structure is in agreement with the absence of halide salts in the crystallization solution of $HheA_{AD2}$. The halide-binding site is formed by two loops extending from the βαβαβ Rossmann fold motif. The first and largest one is equivalent to a highly variable loop that is responsible for cofactor and substrate binding in members of the evolutionarily related SDR family, whereas the second loop corresponds to the Gly-rich cofactor-binding motif of the SDR enzymes (4, 11). The two loops in $HheA_{AD2}$ are almost identical to their equivalents in HheC, with the exception of the region from residue 180 to residue 185. The amino acid sequence of this region in $HheA_{AD2}$ (180-Phe-Asn-Asn-Pro-Thr-Tyr-185) is three residues shorter than that in HheC (178-Leu-His-Ser-**Glu-Asp-Ser**-Pro-Tyr-Phe-186 [the three additional residues are shown in bold]) and has a different amino acid composition. These sequence differences typify the A- and C-type haloalcohol dehalogenases and have important consequences for the way a bound halogen atom or halide ion is stabilized in the two enzymes.

In $HheA_{AD2}$, the water molecule in the halide-binding site interacts with the backbone NH group of Phe180 and the side chain amino group of Asn182 (Fig. 3A). The side chain of Asn182 is kept in position by hydrogen bonds to the carbonyl oxygen atom of Phe180 and to the backbone NH groups of Thr184 and Tyr185. These interactions are facilitated by the sharp turn of the loop at Pro183, which directs the backbone NH groups of Thr184 and Tyr185 inwards. In this way the Asn182 side chain is maintained in a conformation favorable for interaction with a bound halide ion. In HheC, Ser180 is the residue equivalent to Asn182 of $HheA_{AD2}$, but its side chain is ori-

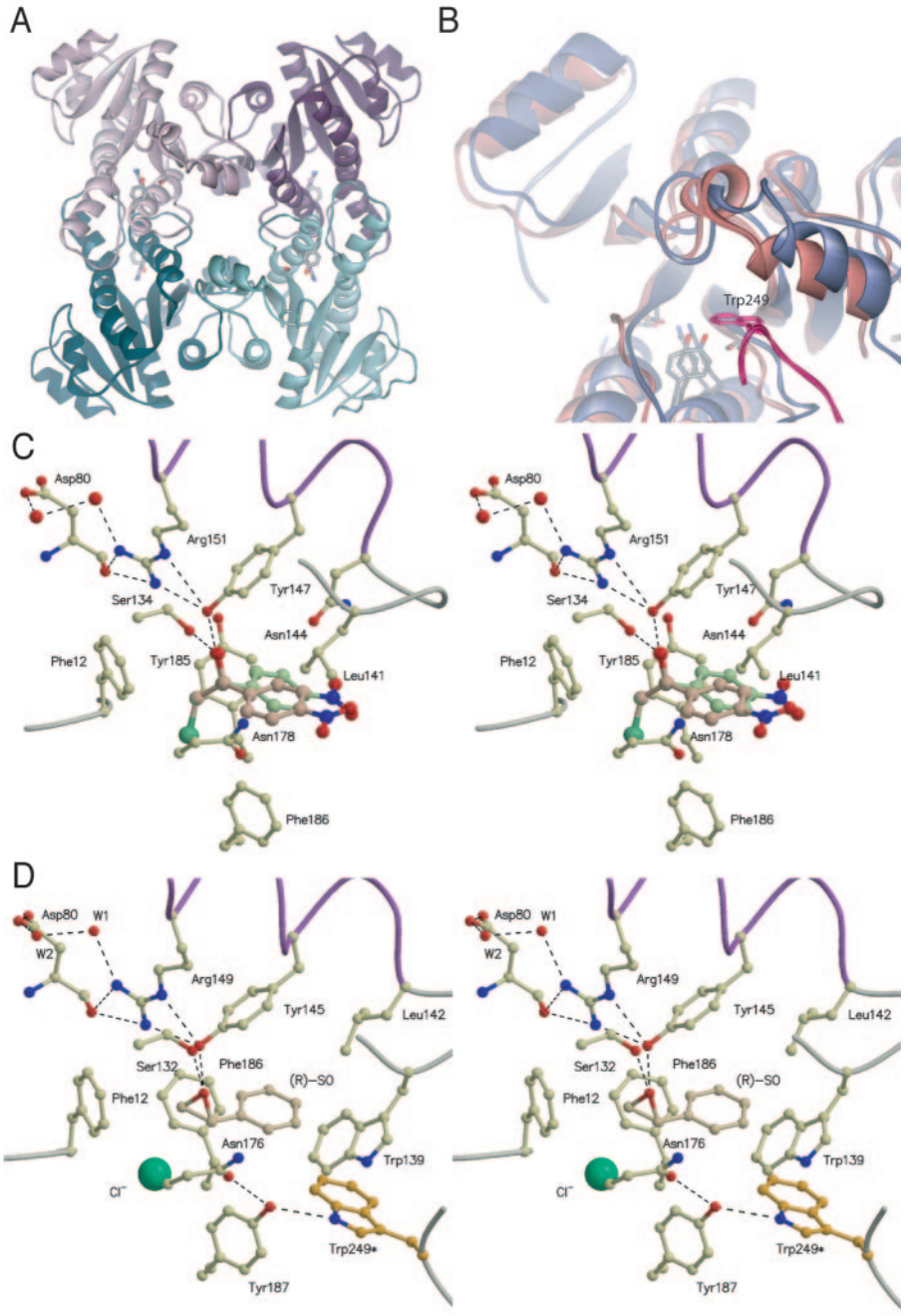

FIG. 2. (A) Tetrameric structure of the haloalcohol dehalogenase $HheA_{AD2}$ from *Arthrobacter* sp. strain AD2. The location of the active site in each monomer is indicated by the catalytic serine, tyrosine, and arginine in stick representation. (B) Close-up view of the superposition of $HheA_{AD2}$ (purple) and HheC (pink), showing the extended C terminus of HheC that contains the side chain of Trp249 that binds in the substrate-binding pocket of an opposite subunit. The catalytic residues are shown in stick representation. (C) Stereo view of the active site pocket of native $HheA_{AD2}$ containing the manually docked *R*-enantiomer (green) and *S*-enantiomer (brown) of the haloalcohol substrate 1-*p*-nitrophenyl-2-chloroethanol. Both enantiomers can be accommodated without severe clashes with the enzyme. (D) Stereo view of the active site pocket of the HheC · Cl^- · (*R*)-styrene oxide (SO) complex (4). Residues, azidoalcohol, and epoxide compounds are shown in ball-and-stick representation, and the chloride ion is shown as a green sphere. Hydrogen bonds are indicated by black dashed lines. Trp249* is contributed by a different monomer in the tetramer of HheC.

ented away from the halide ion (Fig. 3B), which, instead, interacts with a water molecule. This water molecule is hydrogen bonded to the backbone NH group of Phe186 of the *cis* peptide between Tyr185 and Phe186 and the backbone carbonyl group of Leu178, whose atoms are equivalent to the main chain atoms that bind the Asn182 side chain in $HheA_{AD2}$. Thus, part of the large halide-binding loop adopts different conformations in $HheA_{AD2}$ and HheC, which results in local differences in the way the A- and C-type haloalcohol dehalogenases stabilize a bound halogen atom or halide ion.

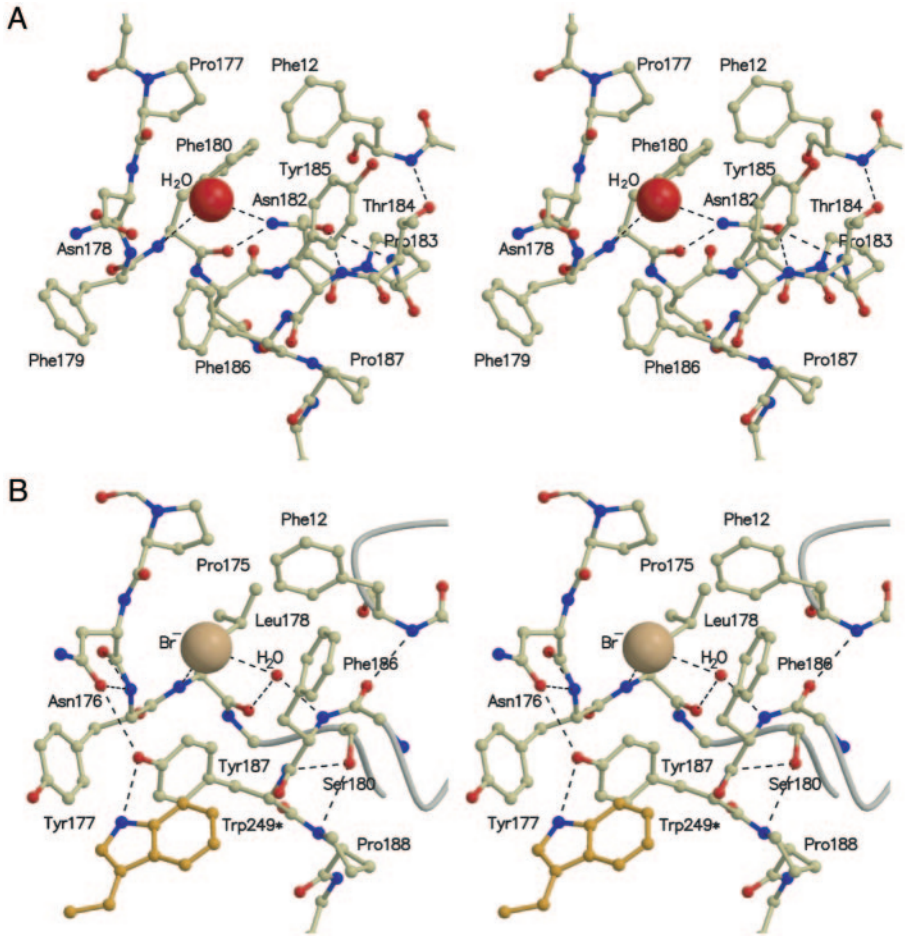

FIG. 3. (A and B) Detailed overview (in stereo) of the halide-binding site in $HheA_{AD2}$ and the HheC · Br^- complex (4), respectively. Residues are shown in ball-and-stick representation, and hydrogen bonds are indicated by black dashed lines. Trp249* is contributed by a different monomer in the tetramer of HheC.

Recently, it was shown for HheC that disruption of two hydrogen bonds between the side chains of Asn176, Tyr187, and Trp249 increases the rate of halide release and can enhance the overall catalytic activity (17). This suggests that in HheC the halide release pathway is near the side chains of these residues. However, in $HheA_{AD2}$, the tyrosine is replaced by a phenylalanine and the tryptophan residue is absent, and therefore further research is needed to establish the halide release pathway in $HheA_{AD2}$.

REFERENCES

1. **Bruns, C. M., I. Hubatsch, M. Ridderström, B. Mannervik, and J. A. Tainer.** 1999. Human glutathione transferase A4-4 crystal structures and mutagenesis reveal the basis of high catalytic efficiency with toxic lipid peroxidation products. J. Mol. Biol. **288:**427–439.
2. **Collaborative Computational Project Number 4.** 1994. The CCP4 suite: programs for protein crystallography. Acta Crystallogr. D **50:**760–763.
3. **de Jong, R. M., and B. W. Dijkstra.** 2003. Structure and mechanism of bacterial dehalogenases: different ways to cleave a carbon-halogen bond. Curr. Opin. Struct. Biol. **13:**722–730.
4. **de Jong, R. M., H. J. Rozeboom, K. H. Kalk, L. Tang, D. B. Janssen, and B. W. Dijkstra.** 2003. Structure and mechanism of a bacterial haloalcohol dehalogenase: a new variation of the short-chain dehydrogenase/reductase fold without an NAD(P)H binding site. EMBO J. **22:**4933–4944.
5. **de Vries, E. J., and D. B. Janssen.** 2003. Biocatalytic conversion of epoxides. Curr. Opin. Biotechnol. **14:**414–420.
6. **Janssen, D. B., J. E. Oppentocht, and G. J. Poelarends.** 2001. Microbial dehalogenation. Curr. Opin. Biotechnol. **12:**254–258.
7. **Laskowski, R. A., M. W. MacArthur, D. S. Moss, and J. M. Thornton.** 1993. PROCHECK: a program to check the stereochemical quality of protein structures. J. Appl. Crystallogr. **26:**283–291.
8. **Lutje Spelberg, J. H., J. E. T. van Hylckama Vlieg, T. Bosma, R. M. Kellogg, and D. B. Janssen.** 1999. A tandem enzyme reaction to produce optically active halohydrins, epoxides and diols. Tetrahedron Asymmetry **10:**2863–2870.
9. **McRee, D. E.** 1999. XtalView/Xfit—a versatile program for manipulating atomic coordinates and electron density. J. Struct. Biol. **125:**156–165.
10. **Navaza, J., and P. Saludjian.** 1997. AMoRe: an automated and improved molecular replacement program package. Methods Enzymol. **276:**581–594.
11. **Oppermann, U., C. Filling, M. Hult, N. Shafqat, X. Wu, M. Lindh, J. Shafqat, E. Nordling, Y. Kallberg, B. Persson, and H. Jörnvall.** 2003. Short-chain dehydrogenases/reductases (SDR): the 2002 update. Chem.-Biol. Interact. **143–144:**247–253.
12. **Otwinowski, Z., and W. Minor.** 1997. Processing of X-ray diffraction data collected in oscillation mode. Methods Enzymol. **276:**307–326.
13. **Read, R. J.** 1986. Improved Fourier coefficients for maps using phases from partial structures with errors. Acta Crystallogr. A **42:**140–149.
14. **Rink, R., and D. B. Janssen.** 1998. Kinetic mechanism of the enantioselective conversion of styrene oxide by epoxide hydrolase from *Agrobacterium radiobacter* AD1. Biochemistry **37:**18119–18127.
15. **Rossmann, M. G., D. Moras, and K. W. Olsen.** 1974. Chemical and biological evolution of nucleotide-binding protein. Nature **250:**194–199.
16. **Tang, L., A. E. J. van Merode, J. H. Lutje Spelberg, M. W. Fraaije, and D. B. Janssen.** 2003. Steady-state kinetics and tryptophan fluorescence properties of halohydrin dehalogenase from *Agrobacterium radiobacter*. Roles of W139 and W249 in the active site and halide-induced conformational change. Biochemistry **42:**14057–14065.
17. **Tang, L., D. E. Torres Pazmiño, M. W. Fraaije, R. M. de Jong, B. W.**

Dijkstra, and D. B. Janssen. 2005. Improved catalytic properties of halohydrin dehalogenase by modification of the halide-binding site. Biochemistry **44:**6609–6618.
18. **Tang, L., J. H. Lutje Spelberg, M. W. Fraaije, and D. B. Janssen.** 2003. Kinetic mechanism and enantioselectivity of halohydrin dehalogenase from *Agrobacterium radiobacter*. Biochemistry **42:**5378–5386.
19. **Terwilliger, T. C.** 2001. Map-likelihood phasing. Acta Crystallogr. D **57:** 1763–1775.
20. **van den Wijngaard, A. J., P. T. Reuvekamp, and D. B. Janssen.** 1991. Purification and characterization of haloalcohol dehalogenase from *Arthrobacter* sp. strain AD2. J. Bacteriol. **173:**124–129.
21. **van Hylckama Vlieg, J. E. T., L. Tang, J. H. Lutje Spelberg, T. Smilda, G. J. Poelarends, T. Bosma, A. E. J. van Merode, M. W. Fraaije, and D. B. Janssen.** 2001. Halohydrin dehalogenases are structurally and mechanistically related to short-chain dehydrogenases/reductases. J. Bacteriol. **183:** 5058–5066.